Chemical Immobilization of Retinoic Acid within Poly(ε-caprolactone) Nanoparticles Based on Drug–Polymer Bioconjugates

Yoon Sung Nam,[1] Kil Joong Kim,[1] Hyung Seok Kang,[1] Tae Gwan Park,[2] Sang-Hoon Han,[1] Ih-Seop Chang[1]

[1]*Amore Pacific R&D Center, 314-1, Bora-ri, Giheung-eup, Yongin-si, Gyounggi-do, South Korea, 449-729*
[2]*Department of Biological Sciences, Korea Advanced Institute of Science and Technology (KAIST), 373-1, Gusung-dong, Yusong-gu, Daejon, South Korea, 305-701*

Received 12 August 2002; accepted 23 October 2002

ABSTRACT: All-*trans*-retinoic acid (RA) was chemically conjugated to biodegradable poly(ε-caprolactone) (PCL_{10}; number-average $M_w \approx 1250$) via an ester linkage. The conjugation was carried out using *N,N*-dicyclohexylcarbodiimide and 4-dimethyl aminopyridine as a coupling agent. The molar ratio of the drug to the polymer was 1.11 as determined by ^{1}H-NMR analysis. DSC and WAXD results showed that the formation of crystalline structures of RA was effectively suppressed by conjugation with PCL. The RA–PCL conjugates were formulated into nanoparticles by a spontaneous phase-inversion technique. Morphological characteristics of the resultant nanoparticles and drug-loading efficiencies were compared with those of free RA-loaded nanoparticles. The drug-loading efficiency of RA–PCL conjugates was almost 100%, while that of free RA was only ~12%. The majority of unconjugated RA was found to form undesirable free-drug crystals out of nanoparticles, as observed by TEM analysis. This study demonstrates that the conjugation approach of RA to PCL can be an effective means to immobilize and encapsulate RA within nanoparticles for pharmaceutical applications. © 2003 Wiley Periodicals, Inc. J Appl Polym Sci 89: 1631–1637, 2003

Key words: biodegradable; polyesters; biological applications of polymers; conjugated polymers; nanotechnology

INTRODUCTION

Retinoids are involved in the proliferation and differentiation of epithelial cells and have been widely used in the treatment of dermatological disorders, such as psoriasis, acne, ichthyosis, and hyperkeratosis.[1,2] It has also been reported that they can induce differentiation and arrest proliferation in a wide spectrum of cancer cells.[3–5] Retinoids are currently used in the treatment of promyelocytic leukemia and are clinically effective as a potential anticancer agent against several types of human cancers.[6,7] However, the precise mechanism of retinoids' biological activity is still under investigation as one of the most important topics in medical sciences.[8,9]

Retinoids are poorly insoluble and chemically unstable in an aqueous medium. Thus, they need to be bound to specific retinol-binding proteins (RBPs) to guarantee their protection, solubility, and transport by body fluids.[10] That is the reason why developing a delivery carrier is a major problem in administrating retinoids as a pharmacological agent. Several methods to produce a delivery carrier for retinoic acid (RA) have been reported: complexation with transthyretin (a natural RBP carrier protein),[11] complexation with cationic polyelectrolytes,[12–16] and encapsulation within liposomes or nanoparticles.[17–19] Complexation of retinoids with transthyretin is a technique to mimic nature's strategy. This is carried out by cocrystallizing RA with a protein, thyroxine-binding transthyretin, which has a high affinity for all-*trans*-RA. However, this technique is an expensive and complicated process. As an alternative approach, Thünemann et al.[12–15] proposed a different and less expensive strategy for the immobilization of RA: the complexation of RA with cationic polyelectrolytes. This approach is based on the formation of ordered structures in solution, which can occur by ionically binding RA to a polyelectrolyte via self-assembly. Although this kind of micellar microcontainer with RA showed interesting physicochemical properties as a new pharmaceutical formulation, the dissociation of the complex in response to environmental changes (e.g., pH and ionic strength) still remains to be examined for practical application. Conventional drug carriers, including li-

Correspondence to: Y. S. Nam (ysnam@pacific.co.kr).

Contract grant sponsor: Ministry of Science and Technology, South Korea; contract grant number: 2000-N-NL-01-C-270.

Contract grant sponsor: Ministry of Education, South Korea; contract grant number: BK21.

Journal of Applied Polymer Science, Vol. 89, 1631–1637 (2003)

posomes and nanoparticles, have also been investigated as delivery vehicles for retinoids. However, physical encapsulation of RA within the drug carriers often causes detrimental free drug crystallization due to the high crystallinity of RA. In this case, the drug should be prevented from diffusing out to the external aqueous phase, which would be followed by its precipitation as a free drug crystal.

Chemical conjugation of RA with a drug carrier is also expected as an alternative immobilization method. Previously, we proposed a new immobilization approach for a wide spectrum of hydrophilic model drugs, such as an anticancer drug,[20,21] an amino acid derivative,[22] a protein,[23] and an oligonucleotide,[24] by chemically conjugating the drugs to a terminal group of biodegradable poly(D,L-lactide-*co*-glycolide) (PLGA). When they were formulated into nano- or microparticles, the drug-loading efficiencies were almost 100% due to the covalent linkage of the target compound to PLGA. In addition, the *in vitro* release profiles of drugs and their PLGA oligomer conjugates from the particulates showed a near-zero order of kinetic behavior over an extended period, while the particulates containing unconjugated drugs demonstrated an initial burst release in the early stage of incubation.

Herein, we report the chemical syntheses and physicochemical properties of RA–polymer conjugates to propose a new immobilization method for RA. All-*trans*-RA is attached onto a biodegradable poly(ε-caprolactone) (PCL) via a biodegradable ester linkage. PCL was chosen because it has been extensively explored for a biodegradable drug-delivery vehicle due to its well-known biocompatibility.[25,26] Differential scanning calorimetry (DSC) and wide-angle X-ray diffractometry (WAXD) were used to characterize whether the conjugation of all-*trans*-RA to PCL affects its crystallization behavior. Furthermore, we investigated the prospects of applying the RA–PCL conjugates to the formulation of polymer nanoparticles.

EXPERIMENTAL

Materials

PLC diols (PCL_{10}) having a number-average molecular weight of 1250 were obtained from Polysciences, Inc (Warrington, PA). All-*trans*-RA and 13-*cis*-RA were purchased from Sigma (St. Louis, MO), and *N*,*N*-dicyclohexylcarbodiimide (DCC), 4-dimethyl aminopyridine (DMAP), and poly(vinyl alcohol) (PVA) with an average molecular weight ranging from 31,000 to 50,000, 87–89% hydrolyzed, from Aldrich (Milwaukee, WI). All other chemical agents were of analytical grade.

Conjugation of RA to PCL oligomer

PCL_{10} (20 mmol based on the number of terminal hydroxyl ends), DCC (25 mmol), and DMAP (1 mmol) were dissolved in 80 mL of anhydrous CH_2Cl_2. RA (20 mmol) dissolved in 20 mL of CH_2Cl_2 was then added to the solution. The coupling reaction was carried out at room temperature for 20 h under mild magnetic stirring. As the reaction proceeded, the color of the solution changed from yellow to orange. After the reaction, the solvent was removed at 30ºC under a vacuum. The resulting product was dissolved in 200 mL of diethyl ether and placed without agitation to precipitate DCC amide. The solution was then filtered and mixed with deionized distilled water under vigorous stirring. An organic layer was separated, dehydrated with $MgSO_4$, filtered through Whatman No.1 paper, and placed at 4ºC to precipitate the RA–PCL_{10} conjugate. This purification was repeated three times. Note that all procedures were conducted under darkness.

Characterization of RA–PCL

The conjugates were characterized by nuclear magnetic resonance (NMR) analysis with a Gemini-300BB NMR. ^{1}H-NMR spectra were taken at 300.06 MHz using a solvent, $CDCl_3$, at 25ºC and chemical shifts were measured in parts per million using $CHCl_3$ (δ = 7.26 ppm) as an internal reference. The conjugation was confirmed by matrix-assisted laser-desorption/ionization time-of-flight (MALDI-TOF) mass spectrometry (Kratos Kompact MALDI II, Kratos, UK). 2,5-Dihydroxybenzoic acid was used as a matrix, which was purified by recrystallization. The conjugates dissolved in acetone were mixed with the matrix at a mol ratio of approximately $1 : 10^3$ on the stainless-steel tip and crystallized immediately before measurement. Mass analysis was carried out with a Voyager DE-STR mass spectrometer equipped with a nitrogen laser emitting at 337 nm. The ions were accelerated at 25 kV with delayed extraction. The conjugates were also analyzed using reversed-phase high-performance liquid chromatography (RP-HPLC). An HPLC system composed of an HP 1100 series (Hewlett–Packard) was used with a C_{18} reversed-phase column (Nova-Pak® C18, 3.9 × 150 mm, Waters) and a 97/3 mixture of acetonitrile and water as an isocratic mobile phase at a rate of 1.0 mL/min. The eluate was monitored by an ultraviolet absorption measurement at 325 nm. DSC analysis was carried out using a TA2010 thermal analyzer instrument (TA Instruments, New Castle, DE). A heating scan was performed at a rate of 10°C/min from −10 to 160ºC. The WAXD patterns were obtained on a powder X-ray diffractometer (D5005, Bruker, Germany).

Nanoparticle preparation

Two types of nanoparticles containing the RA–PCL_{10} conjugate and free all-*trans*-RA were prepared by a spontaneous phase-inversion technique, as reported previously.[20] One hundred milligrams of the RA–PCL_{10} conjugate dissolved in 10 mL of acetone was slowly added to 100 mL of distilled deionized water containing 0.5% (w/v) PVA under vigorous stirring. For the encapsulation of free RA into PCL nanoparticles, 80 mg of PCL_{10} and 20 mg of RA were codissolved in acetone and then used. The nanoparticles formed in the aqueous solution were dialyzed against excess deionized distilled water and then drug crystals were precipitated by centrifugation (Beckman, USA) at 8000 rpm for 30 min. The loading amount of RA within the nanoparticles was determined by an RP-HPLC method. The encapsulation efficiency was calculated based on the percentage ratio of the amount of RA incorporated into nanoparticles to the initial amount used. For observation of the morphology and size distribution, a drop of the sample solution was placed onto a 100-mesh copper grid coated with carbon. After deposition, the grid was tapped with filter paper to remove surface water and negatively stained using a 1% uranyl acetate solution. The samples were air-dried before measurement. Transmission electron microscopy (TEM) was performed on a JEOL 1010 electron microscope (Akishima, Japan). The particle-size distribution was determined using a dynamic laser light-scattering (DLS) technique (Zetasizer 3000HS, Malvern, UK). The scattering angle was fixed at 90° and the temperature was maintained at 25°C. The hydrodynamic mean diameter and polydispersity, μ_2/Γ^2, were calculated by the Contin method.

RESULTS AND DISCUSSION

A schematic synthetic procedure of all-*trans*-RA–PCL (RA–PCL_{10}) conjugates is demonstrated in Figure 1. The ^{1}H-NMR spectrum of the conjugates is given in Figure 2, partly including the ^{1}H-NMR spectrum of the 13-*cis*-RA–PCL_{10} in the insert. 13-*cis*-RA–PCL_{10} conjugates were synthesized and their ^{1}H-NMR spectrum was compared with that of all-*trans*-RA–PCL_{10} conjugates to examine whether the experimental conditions affected the conformation of RA during the conjugation reaction. Note that RA exhibits different biological activities depending on its conformations. ^{1}H-NMR analysis provides a good indicator to discern the conformatinal differences between *cis*- and *trans*-isomers. For example, two peaks appear in the range of 7.7–7.8 ppm for 13-*cis*-RA, while there is no peak for all-*trans*-RA. These peaks are unique for *cis*-isomers. In this study, based on the ^{1}H-NMR spectrum in Figure 2, the isomerization of RA would not occur during the conjugation reaction. This comes as no surprise

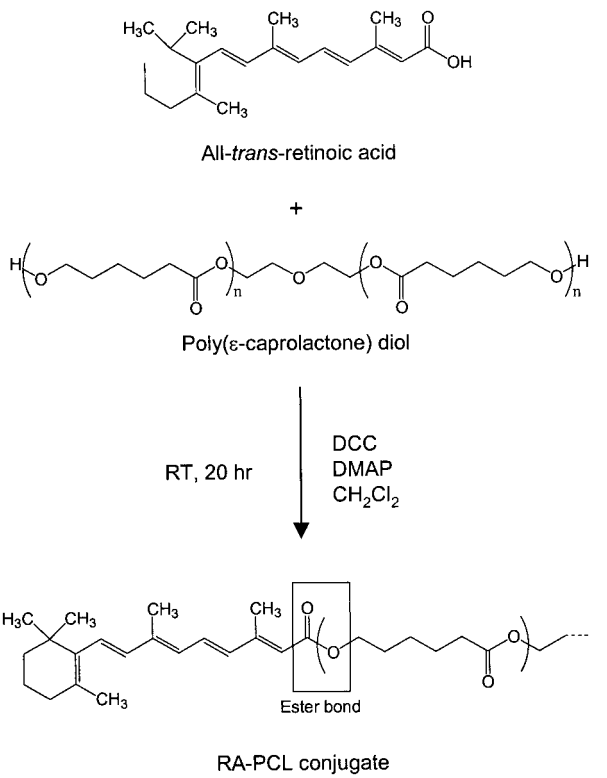

Figure 1 Synthetic scheme of RA–PCL_{10} conjugates.

because much literature has reported the conjugation reaction using retinoids without conformational changes.[27–30] Their conformation is known to be sensitive to high temperature and light, which are not involved in our experimental conditions.[31,32]

From the ^{1}H-NMR spectrum of the RA–PCL_{10} conjugates, it was possible to determine the conjugation efficiency and the conjugation molar ratio by using the relative peak intensity ratio of C$\underline{H}_3$— protons of RA (***1***, δ = 1.05 ppm) to —C$\underline{H}_2$— protons of PCL_{10} (***5***, δ = 4.06 ppm). The weight percentage of the RA moiety in the RA–PCL_{10} conjugate was calculated by the following equation:

$$\text{Weight percent of RA} = \frac{A_{1.05\text{ppm}} \times Mw_{\text{RA}}/6}{(A_{4.06\text{ppm}} \times Mw_{\text{CL}}/2) + (A_{1.05\text{ppm}} \times Mw_{\text{RA}}/6)}$$

where A represents the area of the peak. The molecular weight (Mw) of RA and ε-caprolactone (ε-CL) were 300.4 and 114, respectively. The weight percentage of RA in the conjugates was estimated as 19.2%. These values implicated that 1.11 molecules of RA were conjugated to one main chain of PCL_{10}.

Figure 3 shows reversed-phase HPLC chromatograms of (a) the all-*trans*-RA and (b) the RA–PCL_{10}. The RA–PCL_{10} (retention time = 5.9 min) was eluted much later than was the unconjugated RA (retention time = 2.5 min). This is very reasonable because de-

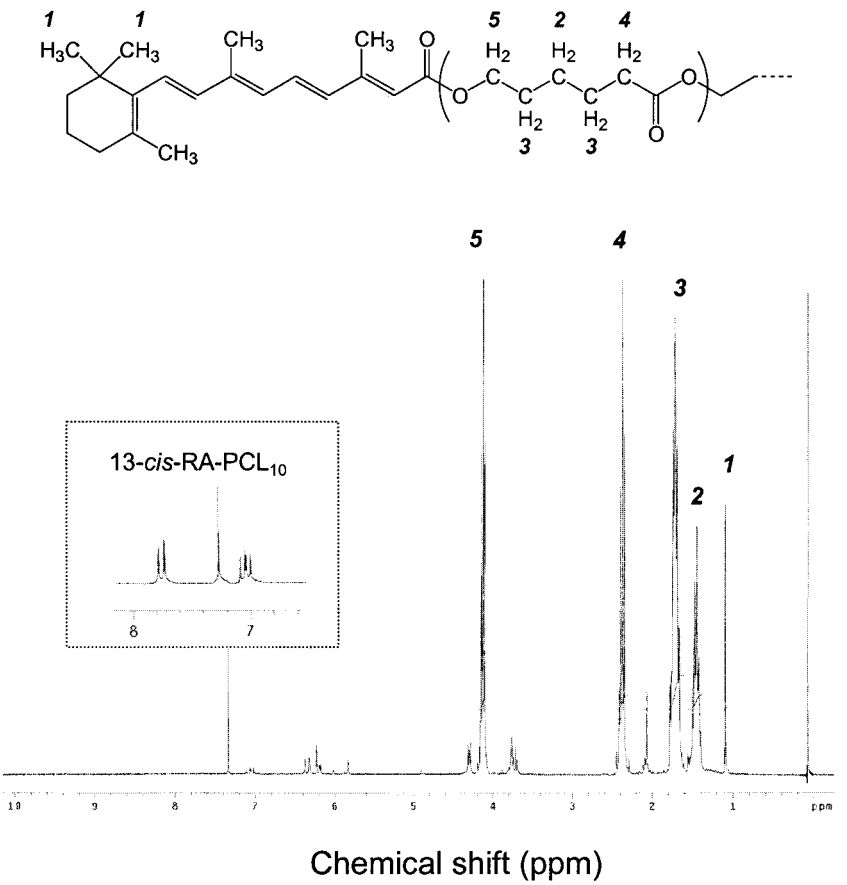

Figure 2 ^{1}H-NMR spectrum, 300.06 MHz, of RA–PCL_{10} conjugates in $CDCl_3$ (all-*trans* form).

layed retention time implies an increase of hydrophobicity as a result of conjugation with PCL_{10}. From the reversed-phase HPLC profile, it was confirmed that free RA was completely removed from the synthesized RA–PCL_{10} sample. The RA–PCL_{10} was additionally analyzed by MALDI-TOF mass spectrometry, which has been widely utilized to determine the molecular weight distribution of synthetic oligomeric polymers.[33,34] Figure 4 shows the MALDI-TOF spectra of PCL_{10} and RA–PCL_{10}, in which well-resolved peaks are detectable. As expected, the repeat unit was 114 Da, which corresponds to the molecular weight of

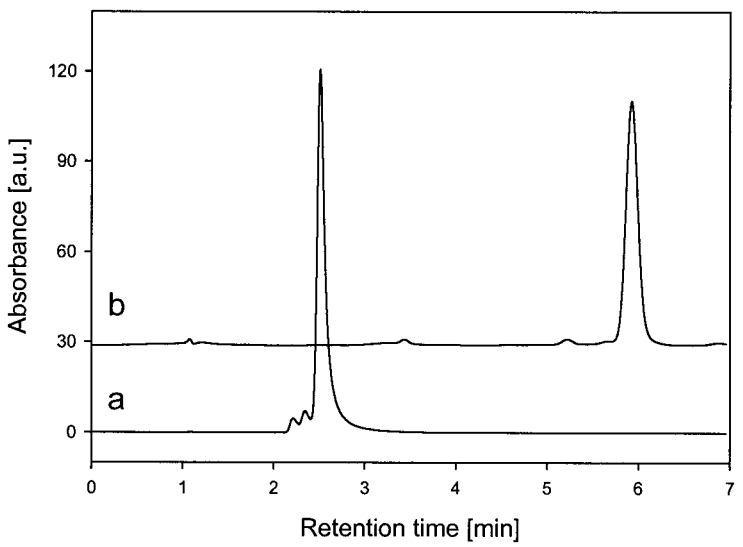

Figure 3 Reversed-phase HPLC chromatograms of (a) all-*trans*-RA and (b) RA–PCL_{10}.

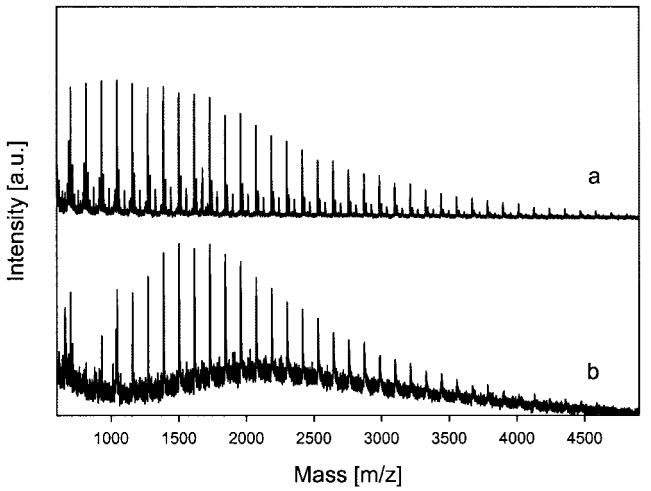

Figure 4 MALDI-TOF spectra of (a) PCL_{10} and (b) RA–PCL_{10}.

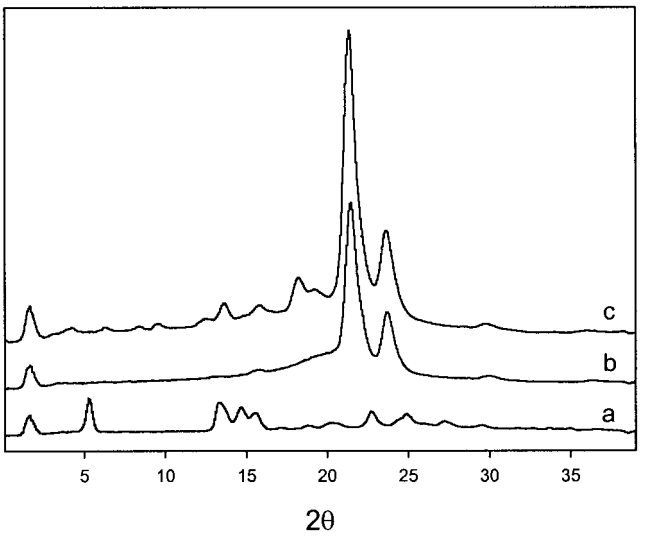

Figure 5 WAXD patterns of (a) all-*trans*-RA, (b)PCL_{10}, and (c) RA–PCL_{10}.

ε-CL. From the measured peak intensities, the number-average molecular weight (M_n), the weight-average molecular weight (M_w), and the polydispersity index (M_w/M_n) were calculated, as shown in Table I. The most probable molecular weight (M_p) of the RA–PCL_{10} conjugates was also compared to that of unconjugated PCL_{10}. The M_p of the RA–PCL_{10} in the mass spectrum was 1501.8, which was larger than that of PCL_{10}, 1043.1, by about 458.7 *m/z*.

Figure 5 shows the representative X-ray diffraction patterns for (a) pure all-*trans*-RA, (b) PCL_{10}, and (c) RA–PCL_{10}. In Figure 5(a), diffraction 2θ peaks at 5.1° and 14.8° are among major angles appearing for the crystalline structure of RA. However, these crystalline peaks could not be observed in the RA–PCL_{10} conjugate in Figure 5(c). In addition, a new peak appeared at $2\theta = 18.5°$. This provides direct evidence that the crystalline structure of RA was destroyed or altered. In Figure 3(c), the typical crystallographic reflections of PCL at $2\theta = 21.0°$ and 24.0°, which agree well with the reported values, still remained in the RA–PCL_{10}. This means that the crystalline structure of PCL has not significantly changed in the conjugates. The DSC results offered more apparent evidence for these structural changes of the RA–PCL conjugates. Figure 6 shows that the representative DSC thermograms for pure RA, crude PCL_{10} powder, and RA–PCL_{10}. The characteristic melting peak of RA at 187.0°C disappeared in the RA–PCL_{10}. The melting temperature (T_m) of PCL_{10} decreased from 57.2 to 50.2°C as a result of RA conjugation. This might be due to a drug-to-polymer interaction, which can preclude the formation of the both the drug and polymer crystalline phases, particularly in rearranging drugs within the polymer network. Based on the WAXD and DSC results, it is clear that the crystallization of RA in RA–PCL_{10} is strictly restricted.

It is of interest to investigate the effect of the altered crystallinities of RA–PCL_{10} on the formation of nanoparticle suspension in an aqueous milieu. Nanoparticles were prepared by a spontaneous phase-inversion and solvent-evaporation method. The TEM observation visibly shows the effect of the RA conjugation with PCL_{10} on the resultant morphology of the prepared nanoparticles. Unfavorable RA crys-

TABLE I
Molecular Weight Distribution of PCL_{10} and RA–PCL_{10} Determined by MALDI-TOF Measurements

Material	M_w	M_n	M_w/M_n
PCL_{10}	1694.3	1439.3	1.18
RA–PCL_{10}	1860.8	1667.4	1.12

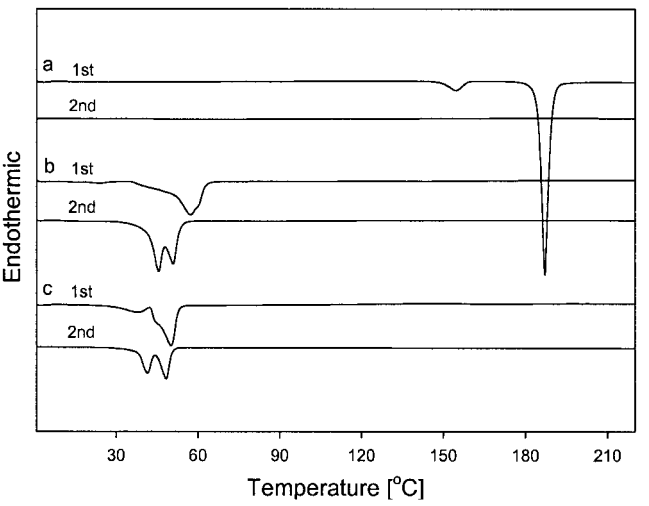

Figure 6 DSC thermograms of (a) all-*trans*-RA, (b) crude PCL_{10} powder, and (c) RA–PCL_{10}.

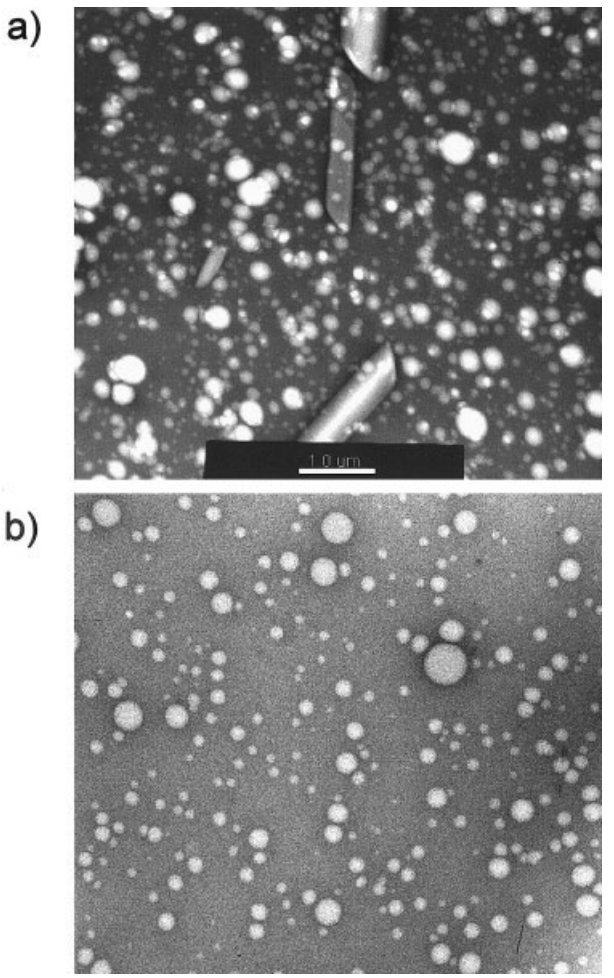

Figure 7 TEM images of (a) free RA-loaded nanoparticles and (b) RA–PCL nanoparticles.

tals were observed in the free RA-loaded nanoparticle suspension, as shown in Figure 7. Most of them were micron-size and distinguishable from spherical polymer nanoparticles. In the RA–PCL_{10} nanoparticle suspension, however, such crystal formation was totally inhibited. From the TEM images, it is conceivable that drug crystallization occurs out of the polymer matrix. Thus, to restrict the unfavorable drug crystallization, RA should be prevented from diffusing out to the external aqueous medium during the particle formation, which would be followed by its precipitation as free drug crystals. This unwanted crystallization often reduces the drug-encapsulation efficiency. In this study, we found that the drug-loading efficiency of RA–PCL_{10} was 99.7%, while that of free RA was only 12.3%, indicating that most of the free RA was removed as a drug-crystal precipitate.

The particle-size distribution and colloidal stability of the RA–PCL_{10} nanoparticles were also determined by DLS. The hydrodynamic mean diameter and polydispersity, μ_2/Γ^2, were 100.8 nm and 0.113 for the blank PCL nanoparticles and 132.3 nm and 0.097 for the RA–PCL_{10} nanoparticles, respectively (Fig. 8). A larger particle size of nanoparticles loaded with drug–polymer conjugates was also observed for doxorubicin–PLGA and doxorubicin–PLGA–PEG conjugates.[20,21] A decreased polymer polarity, resulting from hydrophobic capping of the terminal hydrophilic groups with drugs, is suspected to increase the aggregation number of polymer chains within a particle. As shown in Figure 9, colloidal stabilities of the prepared nanoparticles could be guaranteed for at least 10 days. The results indicate that the RA–PCL conjugate, regardless of the high-loading content of RA, does not affect the colloidal stability of the nanoparticles in an aqueous media.

In conclusion, we have shown that by the chemical conjugation of all-*trans*-RA to PCL highly crystalline all-*trans*-RA could be successfully encapsulated within nanoparticles with a high content of RA moieties, the absence of crystallinity, and greatly enhanced drug-encapsulation efficiency. This study provides a new possibility of an alternative immobilization strategy for retinoids by drug–polymer conjugation.

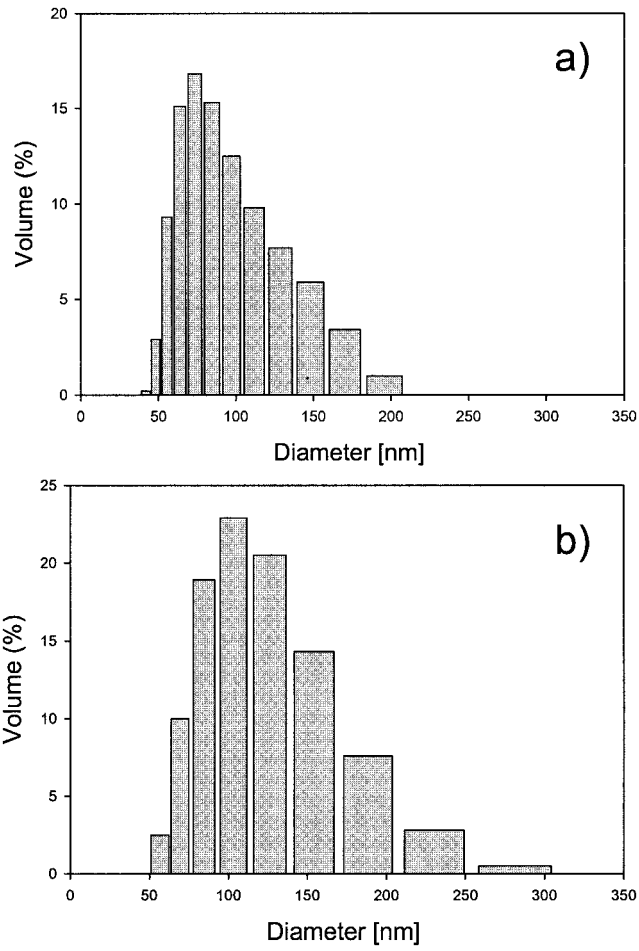

Figure 8 Particle-size distribution of (a) free RA-loaded PCL nanoparticles and (b) RA–PCL nanoparticles.

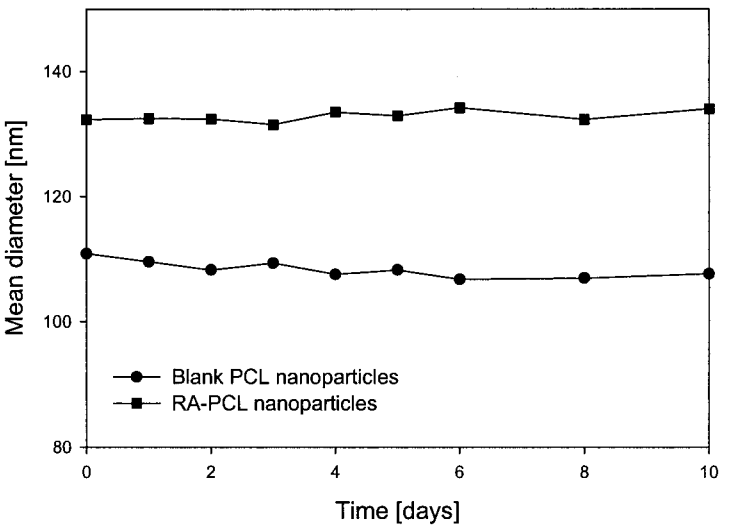

Figure 9 Colloidal stabilities of the prepared nanoparticles in 10 m*M* phosphate buffered saline (pH 7.4, 140 m*M* NaCl) at 37°C for 10 days.

This work was supported, in part, by the National Research Laboratory (NRL) program (Project No. 2000-N-NL-01-C-270) of the Ministry of Science and Technology, South Korea, and the BK21 project of the Ministry of Education, South Korea. The authors would like to thank Su Jung Kim (NICEM) for the TEM analysis and Yun Gyong Ahn (KBSI) for the DSC measurements.

References

1. Gudas, L. J.; Sporn, M. B.; Roberts, A. B. In The Retinoids: Biology, Chemistry, and Medicine, 2nd ed.; Sporn, M. B.; Roberts, A. B.; Goodman, D. S., Eds.; Raven: New York, 1994; pp 443–520.
2. Fritsch, P. O. J Am Acad Dermatol 1992, 27, S8–S14.
3. Niles, R. M. Nutrition 2000, 16, 1084.
4. Breitman, T.; Selonick, S.; Collins S. Proc Natl Acad Sci USA 1980, 77, 2936.
5. Raphaeli, A.; Nordenberg J. Int J Oncol 1994, 1, 481.
6. Castaigne, S.; Chomienne, C.; Daniel, M. T.; Ballerini, P.; Berger, R.; Fenaux, P.; Degos, L. Blood 1990, 76, 1704.
7. Davis, S. M.; Ross, J. A. Med Pediatr Oncol 1999, 32, 49.
8. Minucci, S.; Pelicci, P. G. Cell Dev Biol 1999, 10, 215.
9. Dawson, M. I.; Okamura, W. H. Chemistry and Biology of Synthetic Retinoids; CRC: Boca Raton, FL, 1990.
10. Naylor, H. M.; Newcomer, M. E. Biochemistry 1999, 39, 2647.
11. Zanotti, G.; D'Acunto, M. R.; Malpeli, G.; Folli, C.; Berni R. Eur J Biochem 1995, 234, 563.
12. Thünemann, A. F.; Langmuir 1997, 13, 6040.
13. Thünemann, A. F.; Beyermann, J.; von Ferber, C.; Lowen, H. Langmuir 2000, 16, 850.
14. Thünemann, A. F.; Beyermann, J.; Kukula H. Macromolecules 2000, 33, 5906.
15. Thünemann, A. F.; Beyermann, J. Macromolecules 2000, 33, 6878.
16. Bronich, T. K.; Nehls, A.; Eisenberg, A.; Kabanov, V. A.; Kabanov, A. V. Coll Surf B Biointerfaces 1999, 16, 243.
17. Montenegro, L.; Panico, A. M.; Bonina, F. Int J Pharm 1996, 138, 191.
18. Parthasarathy, R.; Mehta, K. Cancer Lett 1998, 134, 121.
19. Ezpeleta, I.; Irache, J. M.; Stainmesse, S.; Chabenat, C.; Gueguen, J.; PopIneau, Y.; Orecchioni, A. M. Int J Pharm 1996, 131, 191.
20. Yoo, H. S.; Oh, J. E.; Lee, K. H.; Park T. G. Pharm Res 1999, 16, 1114.
21. Yoo, H. S.; Park, T. G. J Control Rel 2001, 70, 63.
22. Oh, J. E.; Nam, Y. S.; Lee, K. H.; Park, T. G. J Control Rel 1999, 57, 269.
23. Nam, Y. S.; Park, T. G. J Microencapsul 1999, 16, 625.
24. Jeong, J. H.; Park, T. G. Bioconj Chem 2001, 12, 917.
25. Gan, Z.; Jim, T. F.; Li, M.; Yuer, Z.; Wang, S.; Wu, C. Macromolecules 1999, 32, 590.
26. Allen, C.; Yu, Y.; Maysinger, D.; Eisenberg, A. Bioconj Chem 1998, 9, 564.
27. Nudelman, A.; Rephaeli A. J Med Chem 2000, 43, 2962.
28. Rho, Y. S.; Kim, W.-J.; Park, S.; Yoo, D. J.; Kang, H. S.; Chung, S.-R. Bull Kor Chem Soc 2001, 22, 581.
29. Harimelahi, G. H.; Ly, T. W.; Yu, S.-F.; Zakerinia, M.; Khalafi-Nezhad, A.; Soltani, M. N.; Gorgani, M. N.; Chadegani, A. R.; Moosavi-Movahedi, A. A. Bioorg Med Chem 2001, 9, 2139.
30. Manfredini, S.; Simoni, D.; Ferroni, R.; Bazzanini, R.; Vertuani, S.; Hatse, S.; Balzarini, J.; De Clercq, E. J Med Chem 1997, 40, 3851.
31. Brisaert, M. G.; Everaerts, I.; Plaizier-Vercammen, J. A. Pharm Acta Helv 1995, 70, 161.
32. Tsunoda, T.; Takabayashi, K. J Soc Cosmet Chem 1995, 46, 191.
33. Thomson, B.; Suddaby, K; Rudin, A.; Lajoie G. Eur Polym J 1996, 32, 239.
34. Liu, J.; Loewe, R. S.; McCullough, R. D. Macromolecules 1999, 32, 5777.